How to cite: *Angew. Chem. Int. Ed.* **2022,** *61,* e202210146
International Edition: doi.org/10.1002/anie.202210146
German Edition: doi.org/10.1002/ange.202210146

Flow Chemistry

On Demand Flow Platform for the Generation of Anhydrous Dinitrogen Trioxide and Its Further Use in *N*-Nitrosative Reactions

*Yuesu Chen, Sébastien Renson, and Jean-Christophe M. Monbaliu**

In memory of Professor Alan R. Katritzky

Abstract: Dinitrogen trioxide (N_2O_3) is a powerful and efficient nitrosating agent that comes with an unprecedented atom economy. However, the synthetic application of N_2O_3 is still underdeveloped mostly due to its inherent instability and the lack of reliable protocols for its preparation. This paper presents an open-source setup and procedure for the on-demand generation of anhydrous N_2O_3 solution (up to 1 M), which can be further used for reactions under batch and flow conditions. The accuracy and stability of N_2O_3 concentration are guaranteed with the absence of head-space in the setup and with the synchronization of the gas flows. The reliability of this protocol is demonstrated by >30 worked examples in the nitrosative synthesis of heterocycles—a library of structurally diverse benzotriazoles and sydnones. Kinetic and mechanistic aspects of the *N*-nitrosative steps are also explored.

Introduction

Nitric oxide (NO) is mostly known either as a common nitroxide pollutant from vehicle exhausts or as a key vertebrate cell messenger. Besides, NO is the primary product of the Ostwald process,[1] and therefore a central intermediate for the industrial production of nitric acid, nitro and nitroso compounds (Figure 1a).[2] Nitrosation is a versatile means of introducing a NO moiety onto organic scaffolds.[3] Although NO is not reactive towards organic molecules in the absence of other reactive species, several downstream products of NO have been employed as nitrosating agents in organic synthesis (Figure 1a).[4] Sodium nitrite ($NaNO_2$)[5] is commonly used as the source of nitrous acid (HNO_2) in nitrosations,[6] whereas alkyl nitrites (R-ONO),[7–9] nitrosyl chloride (Cl-NO),[10,11] and nitrosonium salts (NO^+X^-)[12–14] are employed in anhydrous media. Dinitrogen trioxide (N_2O_3), a powerful nitrosating agent which comes with an appealing atom economy, is frequently involved in NO chemistry under aerobic conditions;[15] it is also believed to be the reactive species in the nitrosation with HNO_2.[16–18] Pure N_2O_3 is a dark blue liquid, which is stable only at low temperature under NO atmosphere.[19,20] Dinitrogen trioxide decomposes spontaneously to NO, N_2O_4, and NO_2 at room temperature[21,22] or upon mixing with a solvent.[23] Nitrosation using pure N_2O_3 is highly exothermic and has to be handled with care under cryogenic conditions.[24] Due to both its instability and high reactivity,

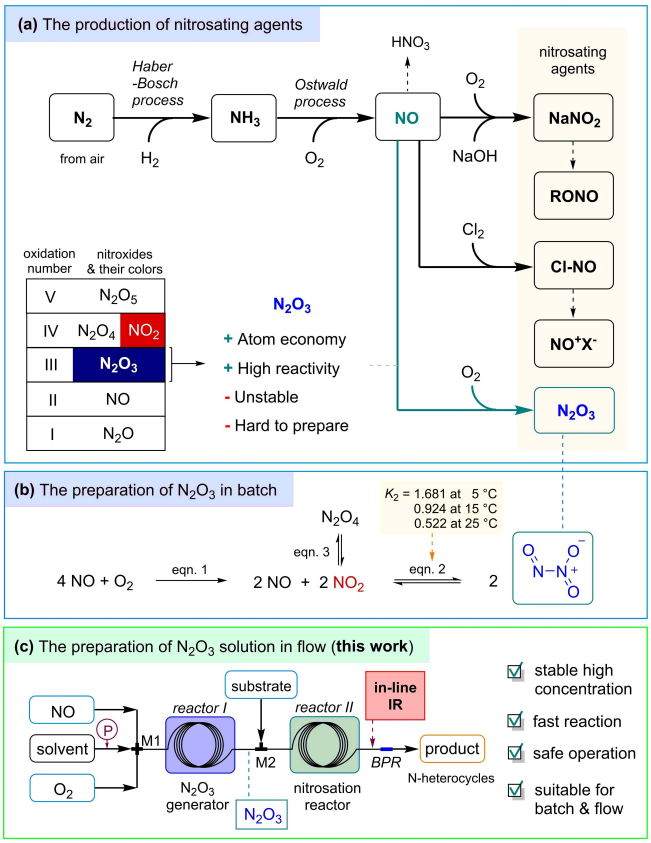

Figure 1. The preparation of nitrosating agents and dinitrogen trioxide (N_2O_3).

[*] Dr. Y. Chen, S. Renson, Prof. Dr. J.-C. M. Monbaliu
Center for Integrated Technology and Organic Synthesis (CiTOS), MolSys Research Unit, University of Liège
B6a, Room 3/19, Allée du Six Août 13,
4000 Liège (Sart Tilman) (Belgium)
E-mail: jc.monbaliu@uliege.be
Homepage: https://www.citos.uliege.be

N_2O_3 is therefore rarely applied as a stock chemical in laboratories and in industry.

Neat N_2O_3 can be prepared with >98% purity by dissolving NO in liquid N_2O_4 at low temperature [Figure 1b, Eqs. (3) and (2)] or by slowly passing an 8:1 (v/v) mixture of NO and O_2 through a cold trap [Figure 1b, Eqs. (1) and (2)].[20] The manipulation of low-boiling toxic compounds requires sophisticated manual operation and is time-consuming because of the slow mass transfer across the gas/liquid (g/l) interface. In some cases, N_2O_3 was generated in situ from $NaNO_2$ and acetic acid[25] or by bubbling NO and O_2 through the substrate solution.[26,27]

In order to utilize N_2O_3 efficiently for organic synthesis, the preparation of its concentrated solution (0.1–1 M) is of practical significance. Bohle and co-workers prepared the N_2O_3 solutions in Brønsted-acid-free media by manually injecting NO and O_2 from gas-tight syringes into a closed test tube containing a solvent at 0 °C.[28] Such operation is slow and cumbersome. It provides only a few milliliters of N_2O_3 solution, and only finds utility for small-scale qualitative experiments, which do not require an accurate concentration of N_2O_3.

The preparation of N_2O_3 solution is always entangled with three problems associated with batch setups. Firstly, mass transport is a persistent issue accompanying g/l reactions. Because of the low solubility of NO[29,30] and O_2[31,32] in organic solvents, the reaction between NO and O_2 mainly takes place in the gas phase. The mass transport across a limited g/l interface renders the operation laborious and time-consuming.[28] Secondly, the gas phase in the head space could influence the composition in the liquid phase. Similar to the preparation of pure N_2O_3,[20] an excess of NO in the gas phase is always required to stabilize the N_2O_3 in the liquid phase, which is wasteful and becomes problematic either upon addition of other reactants or upon workup. Lastly, in the biphasic system, the concentration of N_2O_3 in the liquid phase (c_l) depends on several parameters that are not always independent from one another. Therefore, the individual optimization of the reaction parameters is prohibited by their interrelations.

The g/l mass transport can be accelerated by performing the mixing in a meso- or microfluidic channel.[33,34] The segmented flow pattern in flow channels provides the transport process with immense specific interface,[34,35] which has been successfully exploited for reducing the reaction time of many g/l organic transformations.[36–38]

The phase rule derived by J. W. Gibbs (Figure 2a)[39] can be introduced to elucidate the last two problems.[40,41] This rule relates the number of independent intensive variables (concentrations, temperature, and pressure) (f) in a closed system with the number of independent components (C) and the number of phases (P). There are 5 compounds in a closed system containing an inert solvent and nitroxides with overall composition $NO_{1.5}$ (Figure 2b). Because of the restriction of 2 reactions and 1 constraint, the number of independent components is 2.[40,41] In batch reactors, where the gas phase always exists in the head space (P=2), only 2 among the 4 variables in such system (T and p) can be varied independently (Figure 2c). Regarding the mass

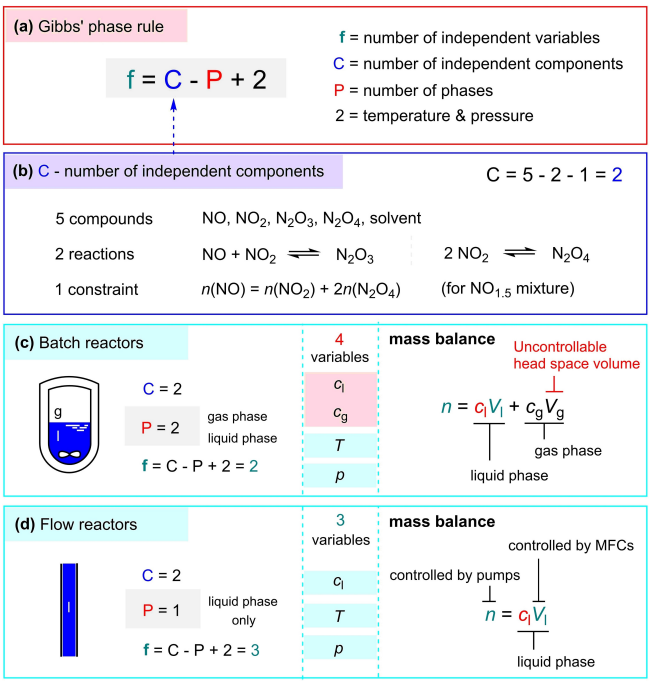

Figure 2. Phase rule and the control of N_2O_3 concentration in the liquid phase.

balance, the concentration in the liquid phase (c_l) is governed by the g/l equilibrium and the volume ratio of the 2 phases. However, the head space volume (V_g), that determines the amount of NO required to stabilize N_2O_3, is usually unknown and difficult to measure. In a flow reactor, where the g/l mixture is continuously moving through a micro-channel, if the gases are dosed in stoichiometric ratio in the formation of N_2O_3 (Figure 1b), the gas phase will disappear after the dissolution of the gases ($V_g=0$, P=1) (Figure 2d). In this manner, 1 variable (c_g) vanishes while 1 degree of freedom (f) is gained, the 3 remaining variables (c_l, T, p) become independent, allowing their individual adjustment during the optimization.

With the aforementioned 3 problems solved by using flow conditions, we could in theory develop a chemical generator[42] to produce N_2O_3 solution from gases and solvent. When the gas phase is eliminated, the N_2O_3 concentration in the liquid phase (c_l) can be precisely controlled by metering devices: V_l by pumps and n by mass flow controllers (Figure 2d). Besides, the continuous flow operation of the generator enables the concatenation with a downstream process that consumes the freshly generated N_2O_3 (Figure 1c). As the gases could be dissolved completely, c_l can be adjusted on the go by tuning the flow rates of both gas feeds without affecting the input flow rate to the downstream reactor.

We herein report our efforts towards a versatile generator of anhydrous N_2O_3 in solution (Figure 1c) along with safe and reliable protocols for its nitrosative reactions. The synthetic utility of N_2O_3 solution is demonstrated through the preparation of the 2 classes of important *N*-heterocycles: benzotriazole (**2**) (Figure 3a) and sydnone (**5**) (Figure 3b).

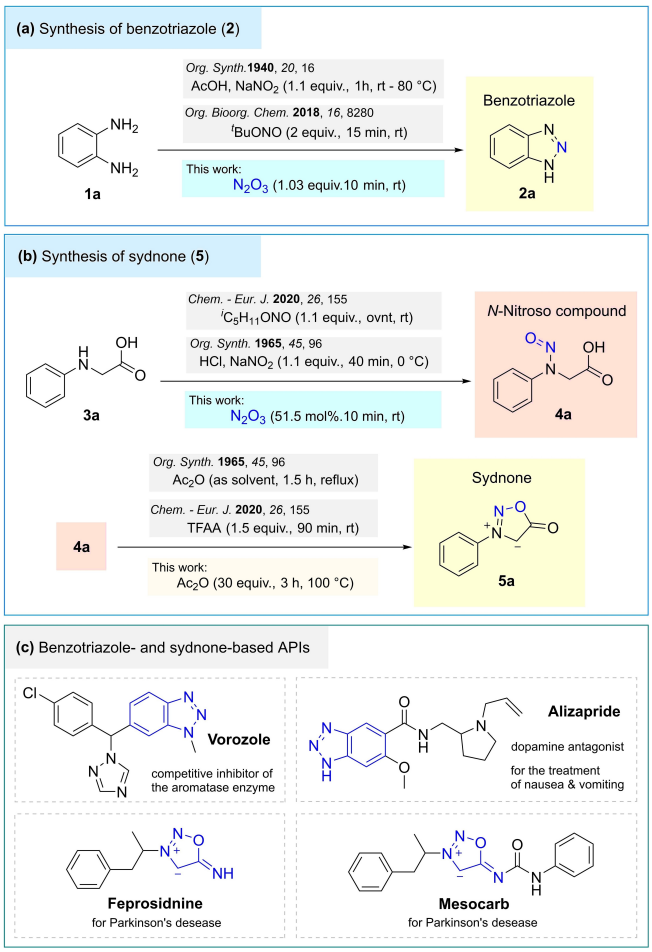

Figure 3. Benzotriazoles and sydnones: synthesis and related APIs.

For both families of *N*-heterocycles, a preliminary *N*-nitrosation of an aniline precursor is the key step. In the prior Art, this step is accomplished either by $NaNO_2$ (ref. **2**;[43,44] **5**[45,46]) or by alkyl nitrite (ref. **2**;[47] **5**[48]). Unsubstituted benzotriazole and its simple derivatives are well established as useful reagents in chemical synthesis,[49–53] especially as peptide coupling reagents.[54–58] Sydnones are mesoionic compounds containing an 1,2,3-oxadiazole ring,[59–61] that have found utility as ligands in organometallic complexes.[62,63] In the synthesis of other *N*-heterocycles, sydnones are often applied as reaction partners in the [3+2] dipolar cycloaddition.[48,64,65] Besides, the benzotriazole and sydnone scaffolds are central to a selection of active pharmaceutical ingredients (APIs) (Figure 3c) and other industrially relevant materials (see below). As both *N*-heterocycles are slightly soluble in water, it will be beneficial to synthesize them in anhydrous media using a volatile nitrosating agent to avoid aqueous workup and extraction.

Results and Discussion

A continuous flow setup for the first trial (Figure 1c) is constructed with commercially available fluidic elements (see Supporting Information for technical details). The reactor coils, injection loops, and other conduits are made from perfluoroalkoxy alkane (PFA) tubing. The pumps and mass flow controllers (MFC) have been calibrated by volumetric methods. The pressure of the flow system is controlled by a membrane back pressure regulator (BPR) and measured with a piezoresitive pressure sensor. An in-line IR spectrometer is connected near the outlet of the flow system to monitor the concentration of N_2O_3.

Nitrogen dioxide was discarded as a gaseous feed stock because of its corrosiveness and high boiling point (21 °C). Instead, we relied on the reaction of NO and O_2 for the generation of N_2O_3. Both gases and an aprotic solvent are brought to contact in an X-mixer (M1) and admixed at 0 °C temperature (reactor I), under which the formation of N_2O_3 is thermodynamically favored (*vide etiam* Figure 1b).[21] When the flow rates of NO and O_2 reaches 4:1 ratio, bubble-free blue solution was observed in reactor I (Figure 4a), yet it evolved to a colorless g/l segmented flow. The alternating mono- and biphasic flow can be attributed to the very different flow rates of two insoluble gases. Because the flow rate of O_2 is only 1/4th of that of NO, O_2 can be blocked by liquid over a longer period of time than NO in response to the change of pressure, releasing a biphasic mixture of NO and solvent (low viscosity) into the reactor coils (Figure 4a). When the O_2 flow resumes, the generated homogeneous N_2O_3 solution (high viscosity) will trigger a new round of pressure fluctuation when it reaches the BPR. Such vicious cycle renders the concentration of N_2O_3 always fluctuating in 5–17 % amplitude (Figure 4b).

After trying out several plausible reactor configurations attempting to generate a homogeneous liquid flow, we moved on with an X-mixer (M1) fitted with two inlet tubing for gases having well-defined internal volumes (the *gas flow synchronizer*) (Figure 4c). These volumes are separated from the upstream by check valves with 2.8 bar back pressure, thus preventing the backflow of the fluid. The internal volumes of the inlet tubing are set proportional to the flow rates of gases ($V_{01}/V_{02}=4:1$). This mathematically derived proportionality [Eq. (5)] maintains the equality of the relative rates of volume changes of the gas phase in these tubing [Eq. (4)], enabling the gas feeds to be blocked and resumed simultaneously in response to pressure variations. As a result of the gas flow synchronization, the flow system is always filled with liquid, which could be either solvent (colorless) or N_2O_3 solution (blue). Since the viscosity-related pressure fluctuation arises from the flow pattern change between two liquids is significantly smaller than that caused by the change between g/l mixture and a liquid, the concentration of N_2O_3 can be stabilized without forming new bubbles (Figure 4d).

Apart from synchronizing the gas flow, additional adjustments were implemented to shorten the startup protocol: since pressurizing the g/l mixture is faster in small reactors, the internal volume of reactor II is made at least 10 times larger than that of reactor I; a six-port valve (6PV II) was inserted in between the two coil reactors for rapid connection and disconnection. When the flow system is thoroughly purged with solvent, reactor II is disconnected

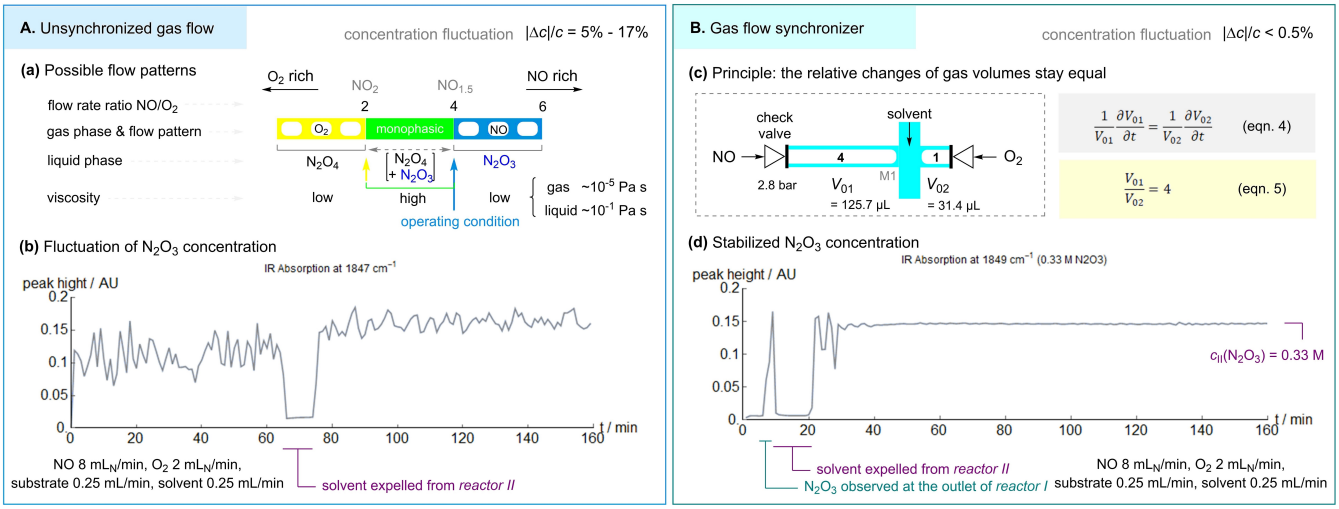

Figure 4. Stabilizing the concentration of N_2O_3 by using the gas flow synchronizer.

by switching the six-port valve before starting the gas supply; after the g/l mixture is pressurized in reactor I to the desired pressure and the blue color of N_2O_3 is observed at the outlet, the reactor II filled with solvent is then switched back to the flow system. This manipulation enables a fast stabilization of the flow pattern (<1 h) by limiting the volume of the gas phase below 9 %. Combining the merits of the gas flow synchronizer and the disconnectable large reactor, the modified flow setup (Figure 5) can be started and stabilized within 40 min, producing homogeneous N_2O_3 solution in a stable concentration (fluctuation <0.5 %) (Figure 4d).

Equipped with a flow setup capable of generating bubble-free N_2O_3 solution with stable concentration (Figure 5), we are able to investigate the property of N_2O_3 solution in organic solvents with process analytical technologies (PAT).[66] As we have discussed previously, the absence of gas phase permits the independent control of the temperature, pressure, and concentration (Figure 2d), the concentration of N_2O_3 is adjustable by changing the flow rate ratio of gas and liquid feeds while maintaining $NO/O_2 = 4$ (Figure 1b); hence, the composition of the dissolved nitroxide is always $NO_{1.5}$ (Figure 4a). The infrared absorption spectrum of the N_2O_3 solution is recorded by an in-line IR spectrometer at different concentrations up to 1 M (Figure 6a). Four peaks corresponding to the vibrations of nitroso and nitro groups in the N_2O_3 molecule can be observed (blue solid arrows in Figure 6a): 1857 cm^{-1} (NO stretching), 1592 cm^{-1} (NO_2 asymmetric stretching), 1298 cm^{-1} (NO_2 symmetric stretching), and 783 cm^{-1} (NO_2 deformation).[67,68] Among them, the peak of the NO stretching (≈1850 cm^{-1}) was used to monitor the concentration of N_2O_3 (Figure 6b, as well as Figure 4b and d), since

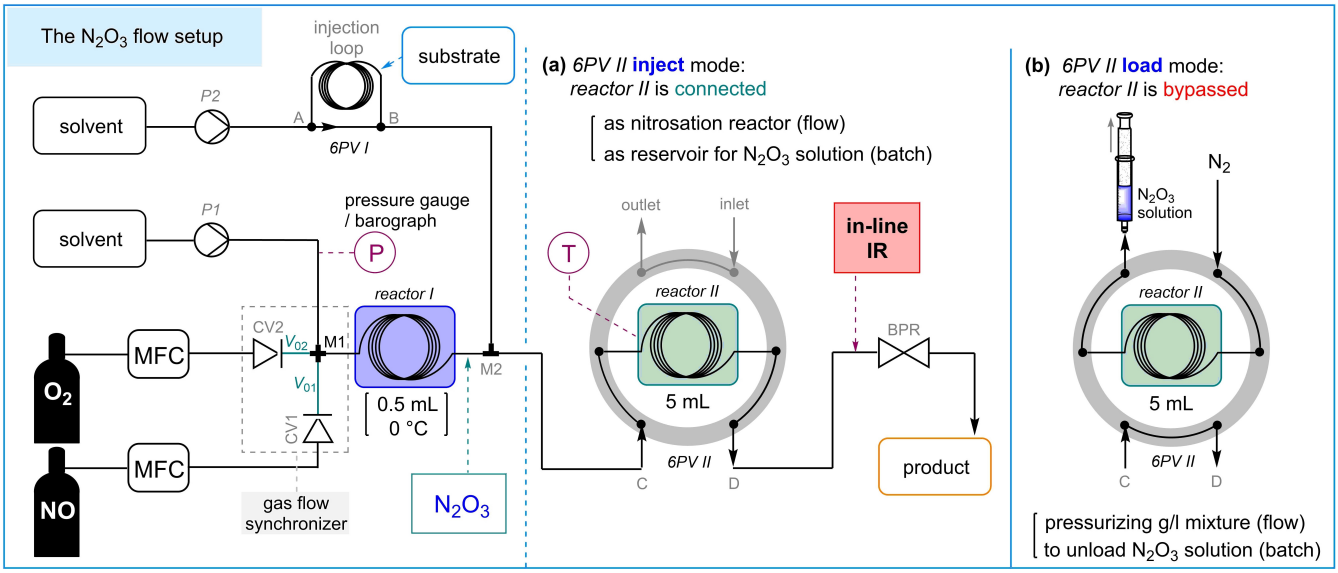

Figure 5. The continuous flow setup for the generation and the reaction of N_2O_3.

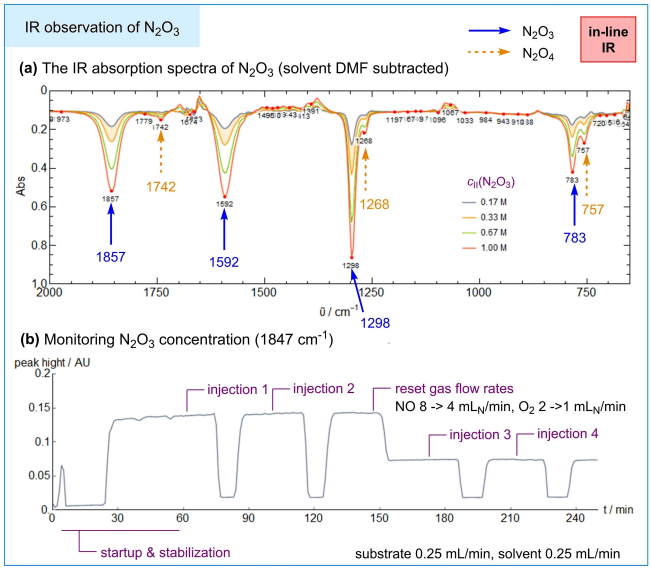

Figure 6. Observation of dissolved N_2O_3 with in-line IR.

it does not overlap with the absorptions of common functional groups in organic molecules. At 20 °C, under which N_2O_3 is thermodynamically unstable (Figure 1b), the peaks of N_2O_4 (orange dashed arrows in Figure 6a)[69] are only visible after subtracting the background absorption of the solvent. Nitrogen dioxide[69] is detectable only under a significant excess of O_2 ($NO/O_2 < 4$, Figure 4a). From the recorded IR spectra (Figure 6a), we can see that dissolved N_2O_3 is quite stable at room temperature in a pressurized monophasic system. The attempt to record the spectra on an FT-IR spectrometer for solid samples failed due to the rapid loss of nitroxides into the atmosphere ($V_g \gg V_l$, $c_g/c_l =$ constant; Figure 2c).

The solution of N_2O_3 is characteristic for its intense blue color, which arises from its absorption of visible light at $\approx$700 nm.[70] The blue color provides a strong contrast to the reaction mixture, which is normally light yellow or colorless, indicating the start- and endpoint in the collection of the product. The water in the solvent could brighten the color of N_2O_3 solution by hydrolysis. The content of water in the solvent was determined by Karl-Fischer titration before carrying out a reaction with N_2O_3. Solvents containing less than 200 ppm of water (a newly opened bottle) were used.

The disconnectability of reactor II enables the flow setup (Figure 5) to be employed for the quantified reactions in both flow and batch. When reactor II is connected (the inject mode, Figure 5a), the substrate solution is injected from the injection loop via a six-port valve (6PV I) and mixed with N_2O_3 solution in the second X-mixer (M2) for the reaction in reactor II. When no substrate is injected, reactor II will be collecting the freshly generated N_2O_3 solution; the solution therein could be collected for batch chemistry by switching the six-port valve (6PV II) to the load mode (Figure 5b) and purging the solution into a dry syringe with nitrogen. The collected solution with known volume is then injected immediately into the substrate solution in a batch reactor. Meanwhile, the N_2O_3 solution is always subjected to positive pressure and minimum exposure to the gas phase; in this manner, the accuracy of N_2O_3 concentration is guaranteed. In the applications in both flow and batch, the stoichiometry can be easily adjusted and precisely controlled by changing flow rates and the liquid phase volume; this feature is not achievable by any existing protocols for the preparation of N_2O_3.

With the operating procedure for the reactions in flow and batch established, we are ready to explore the nitrosation chemistry of anhydrous N_2O_3 solutions (Figure 7). The nitrosation of *o*-phenylenediamine (**1**) can be performed in different aprotic solvents (Figure 7a). Substrate **1b** was converted to the corresponding benzotriazole **2b** in 10 min at 20 °C; the best yield (95 %) was given by acetonitrile (MeCN). A 50:50 (v/v) mixture of dichloromethane (DCM) and MeCN has been employed for some of the *C*-substituted *o*-phenylenediamines (**1g–y**) and their nitrosation products (**2g–y**), which are difficult to dissolve in MeCN alone; *N*,*N*-Dimethylformamide (DMF) appeared as a suitable solvent for most substrates (Figure 8A). Dinitrogen trioxide is so reactive that the reaction completes in 10 min at 0 °C (Figure 7b). We found that 5 bar back pressure is enough to stabilize N_2O_3 solution at 20 °C (Figure 7c). Reducing the pressure to 2.5 bar could result in the formation of gas bubbles and consequently a shorter retention time (t_2). So far, the optimization was performed with 103 mol % N_2O_3; considering the hydrolysis of 1 mol N_2O_3 gives 2 mol HNO_2, we envisaged the stoichiometry of this *N*-nitrosative reaction, seeking the possibility of further enhancing the atom-economy (Figure 7d). The preliminary results in flow turned out to be quite disappointing: 103 mol % N_2O_3 is necessary for a full conversion in 10 min.

In order to explore the reactivity over a longer period, we performed the reaction at 5 °C in a jacketed batch reactor equipped with a digital thermometer. When the solution of 4-methyl-*o*-phenylenediamine (**1p**) was treated with 103 mol % N_2O_3, complete conversion was reached within 5 min (Figure 7e) accompanied by a +24 °C temperature increase (Figure 7f). The reaction with N_2O_3 is very fast and exothermic (cf. ref. [24]), that would be dangerous and difficult to control in large scales in batch.[71,72] When the amount of the N_2O_3 is halved (51.5 mol %), the kinetics exhibits a discontinuous behavior (Figure 7g): ca. 50 % of **1p** was consumed in the first 5 min, and then the reaction proceeded sluggishly over the next 95 min to approach completion. This discontinuity indicates the presence of two nitrosating agents of different reactivity, namely N_2O_3 (0–5 min) and HNO_2 (5–100 min). The reaction with HNO_2 obeys a second order kinetics demonstrated by the linear $1/c-t$ profile (Figure 7h), which means that N_2O_3 is still the active nitrosating species whose formation is rate-limiting.

The nitrosation of *N*-substituted glycines (**3**) was performed in DMF because of their low solubility in many aprotic solvents. The reaction of *N*-phenylglycine (**3a**) with 103 mol % N_2O_3 is fast and clean (Figure 7i). In contrast to **1** (Figure 7d), 51.5 mol % of N_2O_3 is enough to attain a 98 % yield of the *N*-nitroso-*N*-phenylglycine (**4a**) in 10 min (Figure 7j). This stoichiometry was confirmed in the batch experiment (Figure 7k), while a weaker exotherm (+7.5 °C)

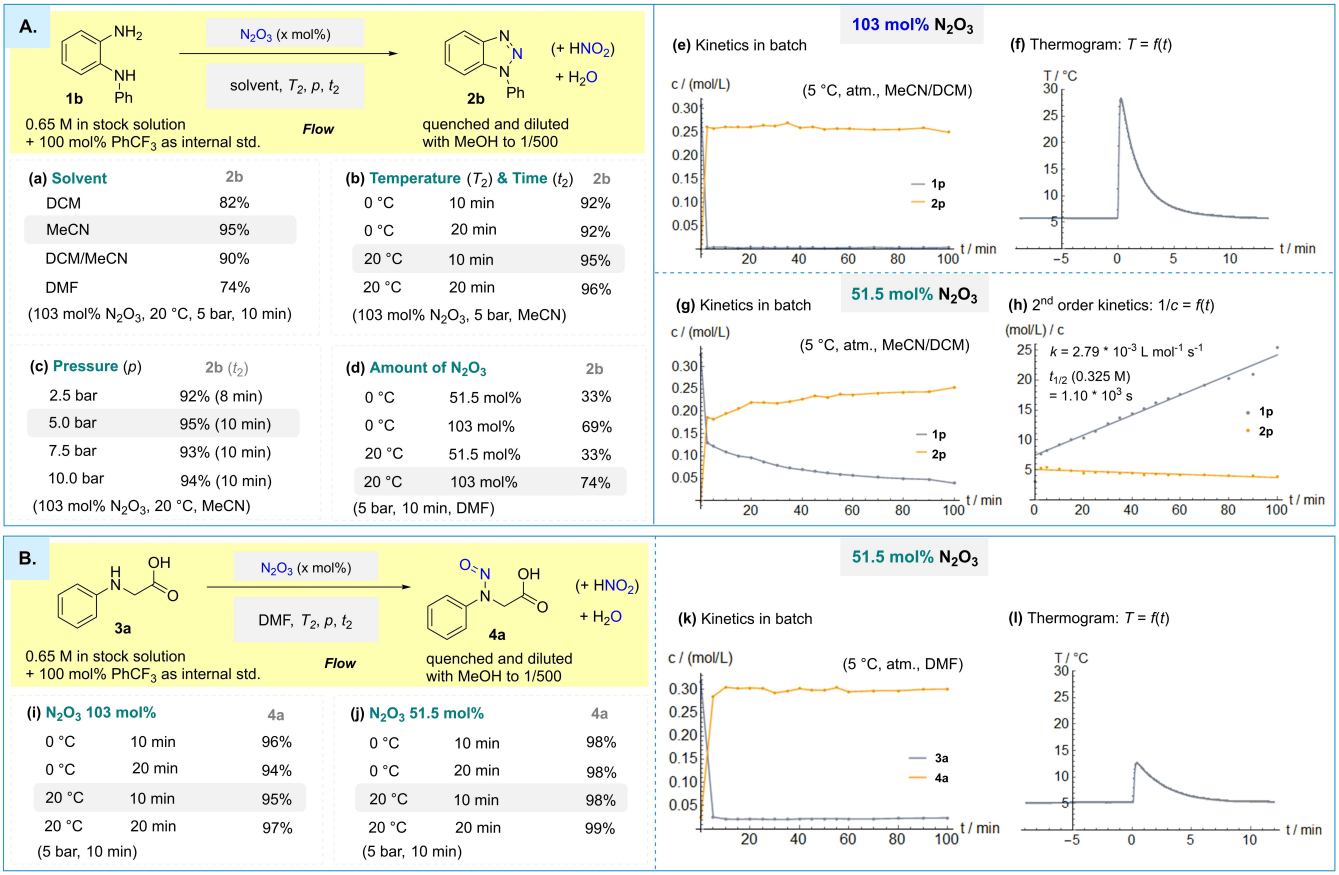

Figure 7. The optimization of reaction conditions: A) the synthesis of benzotriazole; B) the *N*-nitrosation of *N*-phenylglycine. The yields (%) of the products are calculated from the concentrations measured by HPLC-UV (254 nm) with internal standard. For a full list of explored conditions, see Supporting Information.

was observed (Figure 7l). The formation of nitrosyl carboxylate (–COONO) (**3′**) and its subsequent intramolecular *N*-nitrosation[73] are supposed to be responsible for the fast reaction with HNO_2. The nitrosation mixture collected from the outlet of the flow reactor can be directly treated with an acid anhydride without isolating the carcinogenic *N*-nitroso compound (**4**) to afford the sydnone (**5**) (Figure 8B).Using the conditions optimized in Figure 7, a library of benzotriazoles (**2**) and 3-substitued sydnone (**5**) have been successfully synthesized with good yields. The final reaction mixtures were evaporated under reduced pressure and purified by flash chromatography or, sometimes, recrystallization. In the preparation of the unsubstituted benzotriazole (**2a**), the 1 M solution of N_2O_3 has been employed for more concentrated substrate solution (108 g L^{-1}) (Figure 8a).

The substrates in the synthesis of 1-substituted benzotriazoles (Figure 8b) can be prepared from the *N*-functionalization of 2-nitroaniline followed by hydrogenation. This approach provides an alternative to the direct 1-substitution of **2a**. Noteworthy, the acid-sensitive *tert*-butoxycarbonyl (Boc) group (**2e**) survives the treatment with anhydrous N_2O_3 solution, which is similar to the result provided by 2 equiv *tert*-butyl nitrite;[47] whereas the reaction with $NaNO_2$/AcOH gives only deprotected product (**2a**).[47] Generally, the *C*-substituted *o*-phenylenediamines can be cleanly transformed to benzotriazoles (Figure 8c–e). Electron-rich diamine **2o** can be partially oxidized by nitroxides, generating intensely colored sticky side products. Among the synthesized compounds, **2a**,[74–76] **2p**,[77] and **2r**[78] are used as corrosion inhibitors for metals; the structural motives of **2u**, **2v**, and **2y** can be found in the API molecules shown in Figure 3c.

For the synthesis of 3-substituted sydnones (**5**), the *N*-nitrosation step was performed on the flow setup (Figure 5); whereas the cyclization was carried out in batch using conditions adapted from the literature.[45,48] The *N*-aryl glycines (**3**) except **3a** were prepared according to literature procedures (see Supporting Information). Glycine **3a** was converted to the *N*-nitroso compound (**4a**) almost quantitatively by 51.5 mol % N_2O_3 (cf. Figure 7j). Although 103 mol % N_2O_3 could do the same job (cf. Figure 7i), the stoichiometric amount of byproduct HNO_2 will invoke the oxidative degradation of the product in the subsequent step, releasing a red-colored gas (NO_2). After collecting the DMF solution of the *N*-nitroso intermediate (**4**) in a round-bottomed flask, acid anhydride was added to induce ring closure to sydnone (**5**). The reaction of **4** with trifluoroacetic anhydride (TFAA) is fast at room temperature, whereas acetic anhydride (Ac_2O) is much less reactive—it gives no conversion in 1 h at 60 °C. Even though, Ac_2O provides

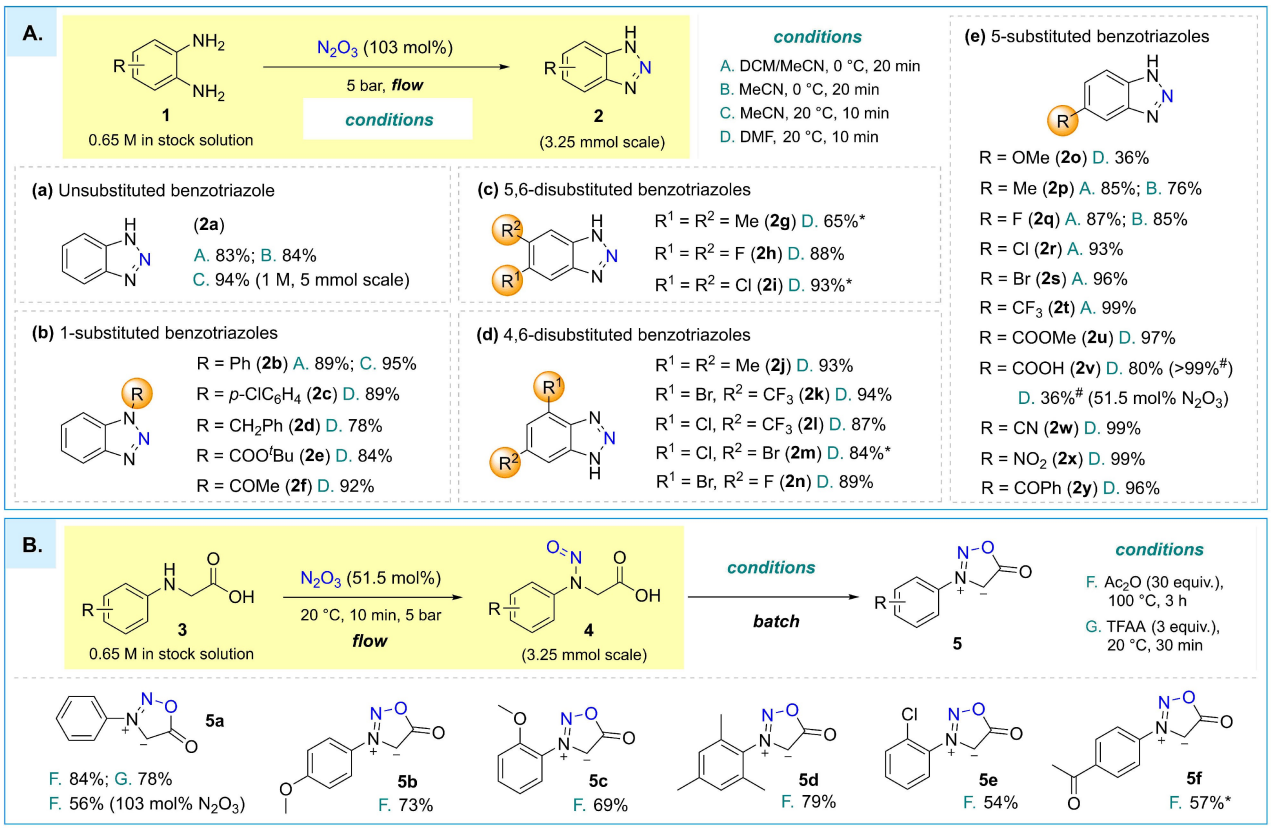

Figure 8. The substrate scope of benzotriazoles (A) and sydnones (B). All yields in this scope are based on isolated pure products after flash chromatography unless otherwise mentioned: *The compound was purified by recrystallization; #the yield is measured by HPLC-UV (254 nm) with internal standard ($PhCF_3$).

good result for **5a** comparable with TFAA. Concerning that DMF (b.p. 153 °C) has to be evaporated after the reaction, Ac_2O is favored in this case because of its mild reactivity as well as its low vapor pressure; while TFAA gives rise to the formation of impurities when the reaction mixture is heated on the water bath.

The mechanistic background of the stoichiometry in the nitrosation of **1** and **3** was investigated in a computational approach. The geometries and the energies of several key transition states (**TS**) have been calculated using Gaussian 16 software[79] (Figure 9C). From the computed molar free enthalpy of activation ($\Delta G_m^{\neq}$), the kinetic constants (k) are calculated (Figure 9A–B). In the reaction of **1a** with N_2O_3 (Figure 9A left), a fast nitrosation takes place on one of the amino groups via a five-membered cyclic transition state (**TS1**);[80,81] the resultant *N*-nitroso intermediate (**1a′**) undergoes dehydration immediately to afford **2a**. However, the byproduct HNO_2 is unable to turnover a second **1a** molecule, since a proton transfer between a base (**1a**) and a Brønsted acid (HNO_2) is more favorable than going through the four-membered ring transition state (**TS2**)[82] towards **1a′**. Therefore, 100 mol % of N_2O_3 is required to complete the conversion in 10 min. In the treatment with 50 mol % N_2O_3 (Figure 7g), the reactivity after 50 % conversion can be attributed to the slow reversing of HNO_2 to N_2O_3.

Regarding the reaction of **3a** with 50 mol % N_2O_3 (Figure 9B), both the amino group and the carboxylic group can be nitrosated by N_2O_3 via cyclic transition states (**TS6** and **TS8**). The primary product of *O*-nitrosation (**3a′**) is unstable and readily rearranges to *N*-nitroso product **4a** via a fast and spontaneous intramolecular process[73] (**TS10**) ($\Delta_r G_m = -19.86$ kcal mol^{-1}), which exhibits no activation barrier. The *N*-nitrosation of **3a** by HNO_2 (**TS7**) is prohibited by a high $\Delta G_m^{\neq}$; the *O*-nitrosation with HNO_2 (**TS9**) is significantly slower than those with N_2O_3, which seemingly cannot account for the fast and quantitative reaction (Figure 7j). The carboxylic group could accelerate the nitrosation with HNO_2 by enabling two processes: the regeneration of N_2O_3 (as Brønsted acid) and the formation of **3a′** (as Lewis base).[73]

In order to find out the process that contributes to the formation of **4a**, compound **1v**, in which the carboxylic group is fixed far away from the amino group, was treated with 51.5 mol % N_2O_3, giving **2v** in 36 % yield (Figure 8e). Since no intramolecular reaction is allowed, the experimental low yield (< 50 %) indicates that the formation of **2v** cannot be promoted by the faster generation of N_2O_3, nor by the accelerated *O*-nitrosation of **1v** (**TS4**) (Figure 9A right). Further computation revealed the existence of a prohibitively high activation barrier ($\Delta G_m^{\neq} = +39.11$ kcal mol^{-1}) in the intermolecular reaction between **1v**

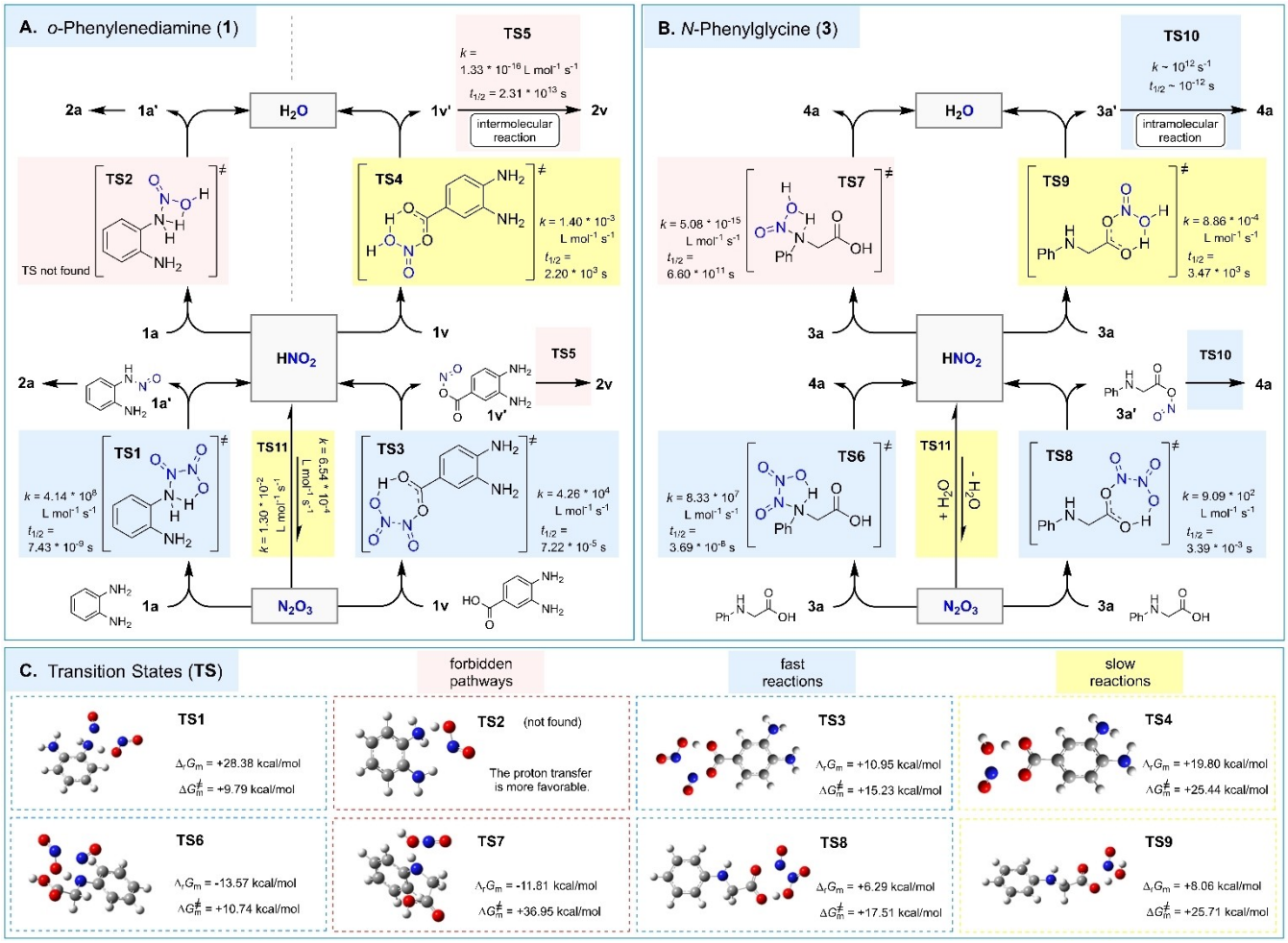

Figure 9. The computational study of the reaction mechanism (M08HX/6-311++G*//B3LYP-D3/6-31+G*, 25 °C in DMF): initial concentration 0.325 M is used in the calculation of the half-lives. For more details, see Supporting Information.

and **1v′** (**TS5**), which ultimately blocks the ways to **2v** via *O*-nitrosation. Consequently, the synthesis of **2v** still requires 100 mol % N_2O_3. Based on the discussion above, we could conclude that the accelerated *O*-nitrosation (**TS9**) with HNO_2 coupled with the intramolecular nitroso migration (**TS10**) permits the fast reaction with HNO_2, requiring only 50 mol % N_2O_3 for the full conversion of **3a** in 10 min (Figure 7j–k).

Computations also show that the hydrolysis of N_2O_3 proceeds very slowly in the presence of 6000 ppm (1 equiv) of H_2O (**TS11**, $t_{1/2}(0.325\,M) = 2.73 \times 10^2$ s). This result accounts for the insensitiveness of the N_2O_3 reactions towards the water in the solvent as well as the water generated from the nitrosative reactions. As experimentally determined earlier (Figure 7h), the rate of the regeneration of N_2O_3 from HNO_2 is approximately 1/10 of the rate of its hydrolysis. A carboxylic group cannot increase the concentration of N_2O_3 to accelerate the overall reaction significantly; as a result, the fast reaction with HNO_2 is almost irrelevant with the regeneration of N_2O_3.

Conclusion

A continuous flow protocol for the generation and reaction of anhydrous dinitrogen trioxide (N_2O_3) solution is presented. Using an open source flow setup and process analytical technologies (PAT) (in-line IR and barometry), concentrated N_2O_3 solution (up to 1 M, 75 g L^{-1}) can be prepared in stable concentration for the nitrosative reactions in flow and in batch. The elimination of head space in the flow reactors enables the independent variation of the reaction parameters (concentration, temperature, and pressure) during the optimization of reaction conditions. Safety concerns associated with the toxic gas and exothermic reactions are minimized by using continuous flow reactors. *N*-Nitrosative steps in the synthesis of two types of N-heterocycles (benzotriazole and 3-substituted sydnone) were accomplished through the efficient and unprecedented use of a stoichiometric amount of N_2O_3, hence demonstrating an elegant and robust technological solution to an unaddressed problem in synthetic organic chemistry. Finally, insights on the reactivity of N_2O_3 and nitrous acid (HNO_2), reaction

mechanism and stoichiometry were provided through a computational study.

Acknowledgements

This work was supported by the "Fonds de la Recherche Scientifique de Belgique (F.R.S.-FNRS)" (Incentive grant for scientific research MIS under grant No F453020F, JCMM). Computational resources were provided by the Consortium des Équipements de Calcul Intensif (CÉCI), funded by the F.R.S.-FNRS under Grant No. 2.5020.11 and by the Walloon Region.

Conflict of Interest

The authors declare no conflict of interest.

Data Availability Statement

The data that support the findings of this study are available in the Supporting Information of this article.

Keywords: Benzotriazole · Continuous Flow · Dinitrogen Trioxide · Nitrosation · Sydnone

[1] L. Hunt, *Platinum Met. Rev.* **1958**, *2*, 129–134.
[2] M. Bertau, A. Müller, P. Fröhlich, M. Kratzberg, *Industrielle Anorganische Chemie*, Wiley-VCH, Weinheim, **2013**.
[3] H.-J. Arpe, *Industrielle Organische Chemie: Bedeutende Vor- Und Zwischenprodukte*, Wiley-VCH, Weinheim, **2007**.
[4] D. L. H. Williams, *Nitrosation Reactions and the Chemistry of Nitric Oxide*, Elsevier, Amsterdam, **2004**.
[5] S. Mukhopadhyay, S. Batra, *Eur. J. Org. Chem.* **2019**, 6424–6451.
[6] R. N. Butler, *Chem. Rev.* **1975**, *75*, 241–257.
[7] A. Dahiya, A. K. Sahoo, T. Alam, B. K. Patel, *Chem. Asian J.* **2019**, *14*, 4454–4492.
[8] N. G. Khaligh, *Mini-Rev. Org. Chem.* **2018**, *17*, 3–25.
[9] P. Li, X. Jia, *Synthesis* **2018**, *50*, 711–722.
[10] L. J. Beckham, W. A. Fessler, M. A. Kise, *Chem. Rev.* **1951**, *48*, 319–396.
[11] R. Lebl, D. Cantillo, C. O. Kappe, *React. Chem. Eng.* **2019**, *4*, 738–746.
[12] L. Bering, A. P. Antonchick, *Tetrahedron* **2019**, *75*, 1131–1143.
[13] G. I. Borodkin, V. G. Shubin, *Russ. Chem. Rev.* **2017**, *86*, 18–46.
[14] N. V. Zyk, E. E. Nesterov, A. N. Khlobystov, N. S. Zefirov, *Russ. Chem. Bull.* **1999**, *48*, 506–509.
[15] M. N. Möller, Q. Li, J. R. Lancaster, A. Denicola, *IUBMB Life* **2007**, *59*, 243–248.
[16] T. A. Turney, G. A. Wright, *Chem. Rev.* **1959**, *59*, 497–513.
[17] L. F. Larkworthy, *J. Chem. Soc.* **1959**, 3116–3122.
[18] J. H. Ridd, *Q. Rev. Chem. Soc.* **1961**, *15*, 418–441.
[19] I. R. Beattie, A. J. Vosper, *J. Chem. Soc.* **1961**, 2106–2109.
[20] A. W. Shaw, A. J. Vosper, *J. Chem. Soc. A* **1970**, 2193–2195.
[21] I. R. Beattie, S. W. Bell, *J. Chem. Soc.* **1957**, 1681–1686.
[22] A. J. Vosper, *J. Chem. Soc. A* **1966**, 1759–1762.
[23] K. A. Rosadiuk, *The Chemistry of Solvated Nitric Oxide: As the Free Radical and as Super-Saturated Dinitrogen Trioxide Solutions*, thesis, McGill University, **2015**.
[24] D. J. Lovejoy, A. J. Vosper, *J. Chem. Soc. A* **1968**, 2325–2328.
[25] L. L. Fershtat, M. I. Struchkova, A. S. Goloveshkin, I. S. Bushmarinov, N. N. Makhova, *Heteroat. Chem.* **2014**, *25*, 226–237.
[26] L. Grossi, S. Strazzari, *J. Org. Chem.* **1999**, *64*, 8076–8079.
[27] M. L. Scheinbaum, *J. Org. Chem.* **1968**, *33*, 2586–2587.
[28] K. A. Rosadiuk, D. S. Bohle, *Eur. J. Inorg. Chem.* **2017**, 5461–5465.
[29] A. W. Shaw, *J. Chem. Soc. Faraday Trans. 1* **1977**, *73*, 1239.
[30] M. H. Abraham, J. M. R. Gola, J. E. Cometto-Muniz, W. S. Cain, *J. Chem. Soc. Perkin Trans. 2* **2000**, 2067–2070.
[31] W. R. Baird, R. T. Foley, *J. Chem. Eng. Data* **1972**, *17*, 355–357.
[32] C. Yong, T. Koichi, O. Takeo, *Bull. Chem. Soc. Jpn.* **1998**, *71*, 651–656.
[33] C. J. Mallia, I. R. Baxendale, *Org. Process Res. Dev.* **2016**, *20*, 327–360.
[34] P. Sobieszuk, J. Aubin, R. Pohorecki, *Chem. Eng. Technol.* **2012**, *35*, 1346–1358.
[35] S. K. Kurt, F. Warnebold, K. D. P. Nigam, N. Kockmann, *Chem. Eng. Sci.* **2017**, *169*, 164–178.
[36] M. B. Plutschack, B. Pieber, K. Gilmore, P. H. Seeberger, *Chem. Rev.* **2017**, *117*, 11796–11893.
[37] C. A. Hone, D. M. Roberge, C. O. Kappe, *ChemSusChem* **2017**, *10*, 32–41.
[38] M. Brzozowski, M. O'Brien, S. V. Ley, A. Polyzos, *Acc. Chem. Res.* **2015**, *48*, 349–362.
[39] J. W. Gibbs, *Trans. Conn. Acad. Arts Sci.* **1878**, *3*, 343–525.
[40] J. S. Alper, *J. Chem. Educ.* **1999**, *76*, 1567–1569.
[41] M. Zhao, Z. Wang, L. Xiao, *J. Chem. Educ.* **1992**, *69*, 539–542.
[42] D. Dallinger, B. Gutmann, C. O. Kappe, *Acc. Chem. Res.* **2020**, *53*, 1330–1341.
[43] R. E. Damschroder, W. D. Peterson, *Org. Synth.* **1940**, *20*, 16.
[44] A. Kokel, B. Török, *Green Chem.* **2017**, *19*, 2515–2519.
[45] C. J. Thoman, D. J. Voaden, *Org. Synth.* **1965**, *45*, 96–99.
[46] S. Kolodych, E. Rasolofonjatovo, M. Chaumontet, M. C. Nevers, C. Créminon, F. Taran, *Angew. Chem. Int. Ed.* **2013**, *52*, 12056–12060; *Angew. Chem.* **2013**, *125*, 12278–12282.
[47] S. Azeez, P. Chaudhary, P. Sureshbabu, S. Sabiah, J. Kandasamy, *Org. Biomol. Chem.* **2018**, *16*, 6902–6907.
[48] S. Specklin, E. Decuypere, L. Plougastel, S. Aliani, F. Taran, *J. Org. Chem.* **2014**, *79*, 7772–7777.
[49] *The Chemistry of Benzotriazole Derivatives: A Tribute to Alan Roy Katritzky* (Ed.: J.-C. M. Monbaliu), Springer Nature, Cham, **2016**.
[50] C. D. Hall, S. S. Panda, in *Adv. Heterocycl. Chem.* (Eds.: E.F.V. Scriven, C.A. Ramsden), Academic Press, Cambridge, MA, 2016, pp. 1–23.
[51] A. R. Katritzky, S. Rachwal, *Chem. Rev.* **2011**, *111*, 7063–7120.
[52] A. R. Katritzky, S. Rachwal, G. J. Hitchings, *Tetrahedron* **1991**, *47*, 2683–2732.
[53] J.-C. M. Monbaliu, L. K. Beagle, J. Kovacs, M. Zeller, C. V. Stevens, A. R. Katritzky, *RSC Adv.* **2012**, *2*, 8941–8945.
[54] A. El-Faham, F. Albericio, *Chem. Rev.* **2011**, *111*, 6557–6602.
[55] A. R. Katritzky, P. Angrish, D. Hür, K. Suzuki, *Synthesis* **2005**, 397–402.
[56] S. B. H. Kent, *Annu. Rev. Biochem.* **1988**, *57*, 957–989.
[57] J.-C. M. Monbaliu, A. R. Katritzky, *Chem. Commun.* **2012**, *48*, 11601–11622.
[58] J.-C. M. Monbaliu, F. K. Hansen, L. K. Beagle, M. J. Panzner, P. J. Steel, E. Todadze, C. V. Stevens, A. R. Katritzky, *Chem. Eur. J.* **2012**, *18*, 2632–2638.
[59] F. H. C. Stewart, *Chem. Rev.* **1964**, *64*, 129–147.

[60] T. Eicher, S. Hauptmann, A. Speicher, *The Chemistry of Heterocycles*, Wiley-VCH, Weinheim, **2012**.
[61] D. L. Browne, J. P. A. Harrity, *Tetrahedron* **2010**, *66*, 553–568.
[62] N. Pétry, T. Vanderbeeken, A. Malher, Y. Bringer, P. Retailleau, X. Bantreil, F. Lamaty, *Chem. Commun.* **2019**, *55*, 9495–9498.
[63] X. Bantreil, N. Pétry, F. Lamaty, *Dalton Trans.* **2019**, *48*, 15753–15761.
[64] E. Decuypère, L. Plougastel, D. Audisio, F. Taran, *Chem. Commun.* **2017**, *53*, 11515–11527.
[65] J. Bouton, S. Van Calenbergh, J. Hullaert, *Org. Lett.* **2020**, *22*, 9287–9291.
[66] J. M. Vargas, S. Nielsen, V. Cárdenas, A. Gonzalez, E. Y. Aymat, E. Almodovar, G. Classe, Y. Colón, E. Sanchez, R. J. Romañach, *Int. J. Pharm.* **2018**, *538*, 167–178.
[67] E. L. Varetti, G. C. Pimentel, *J. Chem. Phys.* **1971**, *55*, 3813–3821.
[68] E. M. Nour, L. H. Chen, J. Laane, *J. Phys. Chem.* **1983**, *87*, 1113–1120.
[69] R. Schaffert, *J. Chem. Phys.* **1933**, *1*, 507–511.
[70] B. A. W. Shaw, A. J. Vosper, P. Polytechnic, B. Road, *J. Chem. Soc. Dalton Trans.* **1972**, 961–963.
[71] B. Gutmann, D. Cantillo, C. O. Kappe, *Angew. Chem. Int. Ed.* **2015**, *54*, 6688–6728; *Angew. Chem.* **2015**, *127*, 6788–6832.
[72] N. Kockmann, P. Thenée, C. Fleischer-trebes, G. Laudadio, T. Noël, *React. Chem. Eng.* **2017**, *2*, 258–280.
[73] R. Gil, J. Casado, C. Izquierdo, *Int. J. Chem. Kinet.* **1994**, *26*, 1167–1178.
[74] M. Finšgar, I. Milošev, *Corros. Sci.* **2010**, *52*, 2737–2749.
[75] Y. M. Youssef, N. M. Ahmed, S. A. Nosier, H. A. Farag, I. Hassan, M. H. Abdel-Aziz, G. H. Sedahmed, *Chem. Pap.* **2020**, *74*, 3947–3956.
[76] H.-S. Lu, X. Zeng, J.-X. Wang, F. Chen, X.-P. Qu, *J. Electrochem. Soc.* **2012**, *159*, C383–C387.
[77] R. Walker, *Corrosion* **1976**, *32*, 339–341.
[78] A. T. Simonović, Ž. Z. Tasić, M. B. Radovanović, M. B. Petrović Mihajlović, M. M. Antonijević, *ACS Omega* **2020**, *5*, 12832–12841.
[79] Gaussian 16, Revision C.01, M. J. Frisch, G. W. Trucks, H. B. Schlegel, G. E. Scuseria, M. A. Robb, J. R. Cheeseman, G. Scalmani, V. Barone, G. A. Petersson, H. Nakatsuji, X. Li, M. Caricato, A. V. Marenich, J. Bloino, B. G. Janesko, R. Gomperts, B. Mennucci, H. P. Hratchian, J. V. Ortiz, A. F. Izmaylov, J. L. Sonnenberg, D. Williams-Young, F. Ding, F. Lipparini, F. Egidi, J. Goings, B. Peng, A. Petrone, T. Henderson, D. Ranasinghe, V. G. Zakrzewski, J. Gao, N. Rega, G. Zheng, W. Liang, M. Hada, M. Ehara, K. Toyota, R. Fukuda, J. Hasegawa, M. Ishida, T. Nakajima, Y. Honda, O. Kitao, H. Nakai, T. Vreven, K. Throssell, J. A. J. Montgomery, J. E. Peralta, F. Ogliaro, M. J. Bearpark, J. J. Heyd, E. N. Brothers, K. N. Kudin, V. N. Staroverov, T. A. Keith, R. Kobayashi, J. Normand, K. Raghavachari, A. P. Rendell, J. C. Burant, S. S. Iyengar, J. Tomasi, M. Cossi, J. M. Millam, M. Klene, C. Adamo, R. Cammi, J. W. Ochterski, R. L. Martin, K. Morokuma, O. Farkas, J. B. Foresman, D. J. Fox, Gaussian, Inc., Wallingford CT, **2016**.
[80] N. H. Morgon, A. R. D. Souza, J. R. Sambrano, *J. Mol. Struct.* **2006**, *759*, 189–194.
[81] Z. Sun, Y. D. Liu, R. G. Zhong, *3rd International Conference on Bioinformatics and Biomedical Engineering iCBBE 2009* **2009**, 10778615.
[82] Y. D. Liu, R. G. Zhong, *Theor. Chem. Acc.* **2009**, *124*, 261–268.

Manuscript received: July 11, 2022
Accepted manuscript online: August 16, 2022
Version of record online: September 2, 2022